Catalytic Model Reactions for the HCN Isomerization. II. Theoretical Investigation of an Anionic Pathway

Fabrice Gardebien* and Alain Sevin

Laboratoire de Chimie Théorique, Université Paris VI, 4, place Jussieu, case courrier 137, F-75252 Paris, France

Received: October 17, 2002; In Final Form: March 14, 2003

A catalytic mechanism is proposed by the present ab initio study for HCN isomerization. This mechanism has to be considered in the context of the reactivity in cometary atmospheres because it supposes the interaction of a cold electron with a hydrated species $HCN{\cdot}H_2O$. The mechanism implies the capture of an electron by the hydrated species and the transfer of the excess energy gained into its internal vibrational modes. The resulting geometry deformation along with the increasing stability against autodetachment for the anionic species can lead to the transition-state structure along the hydrated anionic potential energy surface and can finally lead to the anionic or neutral separated products. The efficiency of this HNC formation mechanism appears then to be dependent on both the water molecule and cold electron densities.

I. Introduction

When comets approach the sun, among the molecules observed in the cometary coma are hydrogen cyanide HCN and its isomer HNC.[1−3] The observed HNC/HCN ratio in Comet Hyakutake is similar to what is found in dense interstellar clouds and is far from the expected equilibrium ratio for the isolated isomerization HCN ⇌ HNC.[3] Because a large fraction of the HNC molecules seem not to be of cometary nucleus origin,[4] there is some need to understand the possible chemical processes occurring in the coma and explaining its formation.

In the present work, we propose a mechanism for the isomerization of HCN to form the less stable isomer HNC. This mechanism takes into account the particular characteristics of the coma—a water-dominated environment and the possible interactions with surrounding electrons of various energies.[5−7]

Both hydrogen cyanide and its isomer are considered in this study to be in a monohydrated form because, on one hand, water comprises the major volatile of the coma (80% for Comet Halley) and, on the other hand, the hydrated HCN complexes are expected to have rather long lifetimes owing to relatively strong intermolecular interactions.[8−11] Electrons are available from the solar wind and are also produced by interactions of parent neutral molecules (mainly H_2O) with solar radiation according to photoionization reactions. The capture of an electron by the neutral monohydrated complex leads to an anionic transient species called a resonant anion.[12−15] Prior to electron ejection, a possible transfer of the excess energy gained upon capture into internal energy can occur if the anion has a sufficiently long lifetime. This energy transfer may lead to overcoming energetic barriers along the hydrated anionic potential energy surface (PES), and this work deals with possible isomerization mechanisms via the hydrated anionic HCN/HNC isomerization barrier.

There exists four monohydrated complexes on the neutral PES of the isomers HCN/HNC, which were previously studied.[8−11] Two of the four complexes have a $HCN{\cdot}H_2O$ global formula and differ in their complexation site: the proton acceptor is either the oxygen, noted as $H_2O{\cdots}HCN$ or the (R) complex, or the nitrogen, noted as HCN···HOH or the (S) complex. The other two complexes of formula $HNC{\cdot}H_2O$ correspond to a hydrogen bond with O for the first one, noted as $H_2O{\cdots}HNC$ or the (P) complex, and with a C atom for the other, noted as HNC···HOH or the (Q) complex. The two neutral complexes HCN···HOH or (S) and HNC···HOH or (Q) have geometries close to the respective anionic reactant and product of the characterized anionic isomerization path. Respective neutral and anionic geometries differ mostly via their ∠HCN/∠HNC value, which is straight in the neutral form and has values of 131.2° and 114.1° values in the anionic complexes $[HCN{\cdot}H_2O]^-$ and $[HNC{\cdot}H_2O]^-$, respectively. Starting from the neutral (S) or (Q) complex, the capture of an electron and the corresponding transition to the anionic PES can be viewed according to two mechanisms. In the first one, the electron capture occurs after the bending of *∠HCN*/*∠HNC* in the neutral complex, which is obtained upon previous vibrational excitation of this mode. The second mechanism implies the bending of the angle induced by electron capture in the optimal neutral geometry. (See the next section.)

One corollary of the well-known Walsh's original rule states that the conformation of a molecule depends to a rather good approximation on its number of valence electrons.[16] A given neutral molecule in its optimal geometry cannot therefore accommodate an extra electron unless subsequent geometric deformations occur. Nevertheless, the electron can be bound temporarily to the neutral molecule by a potential barrier, which results in a combination of Coulombic and centrifugal forces between the incoming electron and the molecular framework leading to the formation of a resonant species.[12−15] From a computational viewpoint, the description of such a transient anion requires a good treatment of the electronic correlation. This requirement is well illustrated by the example of the wave function calculated at the Hartree−Fock level for such systems that places the extra electron into a diffuse molecular orbital (MO). This wave function does not actually describe a resonant state but rather mimics a neutral system and a free electron.

* Corresponding author. E-mail: Fabrice.Gardebien@lct.jussieu.fr. Fax: ++32-65-37-33-66.

10.1021/jp0222393 CCC: $25.00
Published on Web 04/22/2003

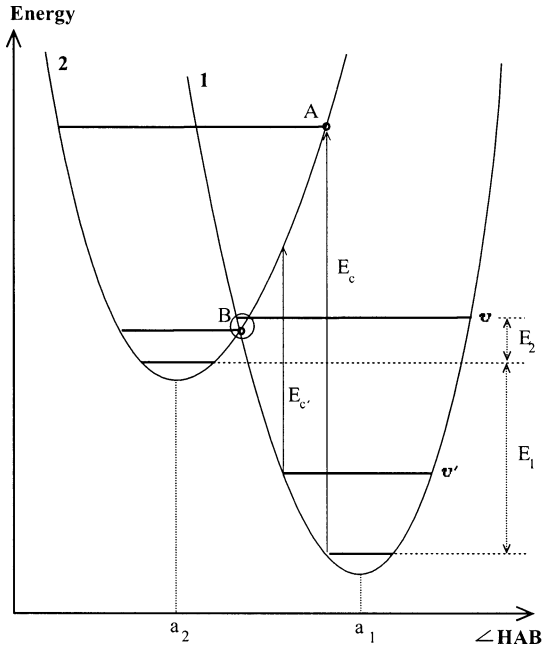

Figure 1. Potential energy curves for the neutral HAB (curve 1) and the anionic HAB^- (curve 2) species in terms of the ∠HAB bending mode. The equilibrium angle value is a_1 for HAB and a_2 for HAB^- (with a_2 taken to be inferior to the a_1 value).

Multideterminant wave functions as obtained with the configuration interaction (CI) method are adequate for the characterization of resonant structures[17−20] because they offer simultaneously a good treatment of the electronic correlation and the opportunity to study the appropriate anionic state. For the characterization of the resonant structures studied here, multireference CI calculations as described in section III were used.

On the ground anionic PES in the regions of fully relaxed geometries, as opposed to steep regions generally associated with the resonance geometries, one can obtain reliable structures and energetics using correlated methods that rely upon a single-determinant reference wave function. Indeed, such theoretical approaches have proven to be able to provide characteristic energies for anions (such as electron affinities or detachment energies) consistent with their experimental counterparts.[21−24] In this paper, all of the neutral and anionic optimal geometries were characterized using second-order Møller−Plesset perturbation theory (MP2),[25] and the energetics were studied using the coupled-cluster method with single, double, and noniterative inclusion of triple excitations (CCSD(T),[26,27] see section III).

The next section describes the proposed mechanisms for the transfer of excess energy into internal modes upon capture. The mechanisms are illustrated with an HAB molecule. Section III presents the computational methods. The results of our calculations are presented in section IV along with a discussion of a mechanism for this proposed hydrated anionic isomerization path.

II. Description of the Proposed Mechanisms

Figure 1 schematically displays potential energy curves of a neutral molecule HAB (curve 1) and its anionic form HAB^- (curve 2) as a function of ∠HAB. Our first scenario for the formation of a metastable anionic HAB^- is as follows. Vibrational excitation of HAB along the ∠HAB bending mode populates the vth vibrational level of the neutral curve; subsequent capture of an electron having negligible kinetic energy leads to the formation of a transient negative ion HAB^-*. If this anion is long-lived enough, a redistribution of the excess internal energy E_2 among internal vibrational modes can occur. In the second capture mechanism, the incoming electron has the kinetic energy E_c, and its capture by neutral HAB in its lowest vibrational state leads to an anionic species that starts to vibrate around the a_2 equilibrium-angle value of HAB^-, provided that the excess energy $E_c - E_1$ is transferred into the internal vibrational modes.

The probability of electron capture is proportional to the Franck−Condon factor, which is maximal at point B for the first mechanism and at point A for the second mechanism. Other cases that are intermediate between these two limiting mechanisms are likely and correspond to an initial neutral structure with vibrational internal energy $E_{v'}$ distributed along the ∠HAB bending mode. The subsequent capture of an electron with incident kinetic energy $E_{c'}$ may lead to vibrationally excited HAB^-*. The probability for negative ion formation from vibrationally excited states is enhanced as a result of the larger Franck−Condon region of the vibrationally excited molecules.[12]

As when dealing with the dissociative attachment process of sufficiently long-lived anions, where the excess energy gained upon attachment is distributed into internal vibrational modes and then into kinetic energies for the separating fragments,[28−30] the above-described mechanisms are found upon initial attachment and imply a conversion of the excess energy into internal vibrational energy. This energy conversion and the resulting vibrational energy redistribution is due to strong coupling between a few vibrational modes and the anionic electronic state and may result in nondissociative electron attachment, particularly in large molecules or in complexes.[22,31,32] When the total energy is maintained (this is the case for regions of low density that provide a small probability of collision), a redistribution of this energy may provide sufficient internal energy to overcome potential barriers on the anionic PES, but the required activation energy must be less than the internal energy gained upon attachment. It should be stressed that, in all cases, competition exists between electron attachment and its ejection (autoionization).

III. Methodology

All geometry optimizations were achieved using the Møller−Plesset second-order perturbation theory (MP2)[25] as implemented in the program system Gaussian 98.[33] The 6-311+G**[34−36] basis set was used during the geometry optimizations to determine all minima of the neutral and anionic PESs as well as the anionic transition state. Single-point calculations were repeated on the stationary points with the coupled-cluster method with single, double, and noniterative inclusion of triple excitations (CCSD(T)[26,27]) and using the 6-311+G(3df,2p) basis set. A correlated wave function is needed to account for the important correlation energy in these systems.[37,38] We have reported the CCSD(T)/6-311+G(3df,2p) energies including zero-point energy (ZPE) and basis set superposition error (BSSE) corrections. The counterpoise method of Boys and Bernardi[39] was used to correct for the BSSE. The ZPE correction was calculated using the frequencies calculated at the MP2/6-311+G** level for the neutral (closed shell) stationary points and at the B3-LYP/6-311+G** level for anionic (open shell) species. The former method results in less reliable ZPEs than the latter when treating open-shell species.[40] The ZPE correction was made using the scaled harmonic vibrational frequencies. The appropriate scaling factors were taken from a study by Scott and Radom.[41] The MP2 method with a sufficiently large basis set has proven to be relevant for

the optimization of both neutral and anionic complexes.[22,42−44] The unrestricted formalism (UMP2 and UCCSD(T)) was used for the open-shell anionic systems. In the basis set, diffuse functions are essential in evaluating anionic barriers;[45−49] however, diffuse functions on the hydrogen atoms are not required for a proper description of the valence anions.[45,47] Spin contamination was found to be small for the calculated anionic species. The reported charges are taken from the Mulliken population analysis of the optimized structures. For the minima, we have verified that all eigenvalues of the respective Hessian matrix had positive values and that the Hessian matrix of the transition state had only one negative eigenvalue. The connections between the anionic transition state and the two anionic complexes were confirmed by performing intrinsic reaction coordinate (IRC) calculations[50,51] near the transition-state region followed by geometry optimization of both the reactant and product. The vertical detachment energy (VDE) is defined as the energy difference between the ground-state anion and the corresponding neutral system retaining the anion structure. Our VDEs are calculated at the CCSD(T)/6-311+G(3df,2p) level by subtracting the energy of the anion from that of the neutral having the equilibrium geometry of the anion. This energy difference takes into account the ZPE corrections for both anionic and neutral forms as well as the BSSE corrections when necessary (complexes AR and AP only). A positive VDE value indicates that the corresponding anion is stable against autodetachment and suggests that such an anion should be relatively long-lived. As an example, a positive VDE was calculated for relaxed bent CO_2^-;[52,53] this result is consistent with its measured, rather long lifetime of $\sim$90 μs with respect to autodetachment.[54] Correlated methods based upon a single-determinant reference wave function have proven to be accurate enough by reproducing experimental positive VDEs.[21−24] Conversely, negative VDE values indicate very short-lived anions, and more sophisticated methods are normally required if one aims to determine precise VDEs. However, in this study, our purpose was not to have refined VDEs but rather to derive reasonably accurate values to predict the stability of the relaxed anion geometries toward electron detachment.

To characterize the resonant hydrated complexes and to obtain the electron attachment energies, multiconfigurational calculations were achieved with the MOLPRO code.[55] Multiconfigurational calculations yield reliable results for the description of resonant species.[17−20] The resonant species were characterized with the internally contracted multireference CI method,[56−59] including all single and double excitations relative to any of the reference configurations and using the 6-31+G** basis set. The attachment energy associated with the formation of a resonant anion is the energy difference between the anion and the corresponding neutral optimized nuclear configuration. We took advantage of the planar geometries obtained for complexes (S) and (Q) by calculating the corresponding attachment energy in the C_s group. The first resonant state of both complexes is then either one of two degenerate states 2 ^{2}A′ or 1 ^{2}A″. We choose to characterize the 1 ^{2}A″ state for (S) and (Q). Furthermore, because for the attachment energies of both complexes nondynamical correlation effects are not expected to be important, only the highest occupied molecular orbitals each of A′ and A″ symmetry (respectively 10a′ and 2a″) were included in the active space. The four lowest virtual MOs of A′ symmetry and the two lowest virtual MOs of A″ symmetry were also included in the active space (from 11a′ up to 14a′ and 3a″ and 4a″, respectively). The MOs that are used are the natural orbitals taken from a previous MRCI calculation. We ensured that the method that was used was reliable by reproducing the experimental attachment energy for the first resonant state of HCN, which is of the same nature as for hydrated HCN: in both cases, the extra electron is described by the same type of orbital (π^*_{CN}).

IV. Hydrated Anionic Isomerization

To our knowledge, no study exists on the degree of hydration of the molecules HCN and HNC in cometary atmospheres. The degree of hydration of these molecules likely varies with the distance from the icy surface of the cometary nucleus because the potentially formed structures may result from two opposite trends. Indeed, the great proportion of water in the bulk ice favors highly hydrated complexes right from the sublimation (therefore, mostly in the vicinity of the nucleus) whereas the interactions with solar radiation would split the formed complexes into smaller units (at larger distance from the nucleus). In this study, we will assume an interaction of an electron with a monohydrated form of HCN.

On the neutral monohydrated PES of HCN, one complex, (R), exists that is more stable by 0.02 eV than complex (S). If one considers that the ambient conditions allow the formation of monohydrated species, then the thermodynamic complex (R) that would be initially formed would also be in the presence of the (S) structure owing to the high-temperature condition (200 K is the expected near-nucleus coma temperature) in the inner part of the coma. (A small barrier is assumed to exist between (R) and (S) because only the weak hydrogen bond is perturbed along the path connecting these two complexes, thus inducing only small energy variations.)

On the anionic PES, two complexes (AR) and (AP) were determined (Figure 2). We have verified with an IRC calculation that these complexes were connected to the anionic isomerization transition state (AT). The asymptotic limits $HCN^-/HNC^- + H_2O$ of this surface were also characterized, but they are not of interest for the discussion of the possible mechanisms. In this section, we will discuss the geometric and energetic characteristics of the determined hydrated anionic isomerization path.

A. Structures. 1. Complexes. Figure 2 presents the geometries of the two anionic complexes (AR) and (AP). The two neutral complexes closest in geometry, (S) and (Q), are also presented.

In the anionic complexes, the negative charge is essentially localized on the HCN or HNC fragment ($\gtrsim$96%) and is shared by the C and N atoms, thus showing that the H_2O moiety does not bear significant charges. These structures will be noted as $HCN^-\cdots HOH$ and $HNC^-\cdots HOH$ in the text. In these two H-bonded species, strong electrostatic interactions arise from the charge localization. In both cases, the hydrogen bond is close to being linear ($\angle$O4H5$\cdots$N = 169.1°, $\angle$O4H3$\cdots$C = 164.2°), and the corresponding distances N$\cdots$H5 and C $\cdots$H3 are 1.762 and 1.929 Å, respectively. The OH bond of H_2O forming the hydrogen bond is elongated by 0.043 Å in $HCN^-\cdots HOH$ and by 0.037 Å in $HNC^-\cdots HOH$ with respect to free H_2O. The harmonic vibrational frequencies have been calculated for the two complexes. The calculations predict significant frequency shifts for the symmetric OH stretching mode in both complexes with respect to free H_2O, the frequency being reduced by 708 and 615 cm^{-1} for $HCN^-\cdots HOH$ and $HNC^-\cdots HOH$, respectively. The lengthening of the OH bonds and the resulting large red shifts for the stretching frequencies are consistent with the formation of strong hydrogen bonds.

Despite the smaller charge on the N-atom end (−0.54*e* in $HCN^-\cdots HOH$) than on the C-atom end (−0.74*e* in

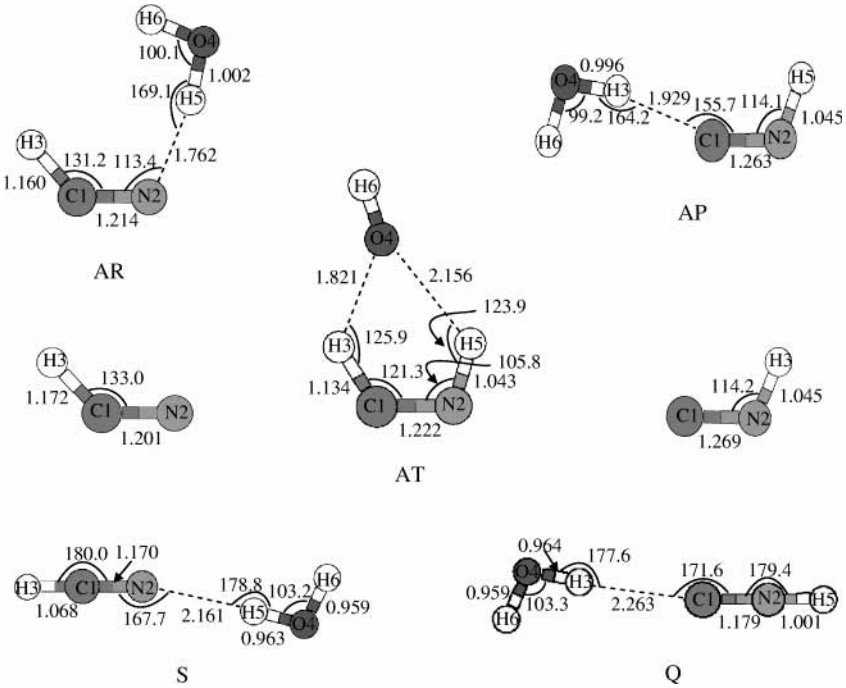

Figure 2. Geometries of the anionic reactant (AR), anionic product (AP), anionic transition state (AT), and isolated species HCN^- and HNC^- determined at the MP2/6-311+G** level. Geometries of neutral complexes (S) and (Q) are also reported. Bond lengths are in angstroms, and angles, in degrees.

$HNC^-\cdots HOH$), on the basis of the geometrical features for the two H-bonds (OH bond elongations, C···H3 and N···H5 length differences) and vibrational perturbations of the OH bond, one would expect a greater complexation energy for the complex $HCN^-\cdots HOH$. However, our calculations give a smaller complexation energy value for $HCN^-\cdots HOH$ (0.63 eV) than for $HNC^-\cdots HOH$ (0.67 eV). An explanation comes from the diffuseness of the electron density around the N and C atoms in the HCN^-/HNC^- charged moiety: the nitrogen, being more electronegative than carbon, has its electron density localized closer to the nucleus whereas the space spanned by the carbon electron density is wider. In the nitrogen case, the more localized charge contributes to stronger electrostatic forces and then contributes to greater perturbations of the OH bond length and stretching frequency and to a smaller intermolecular distance.

The structural parameters for the HCN^- moiety in $HCN^-\cdots HOH$ deviate very slightly from those of free HCN^-. The same remark applies to the HNC^- part of $HNC^-\cdots HOH$. An examination of the dihedral angles shows that both complexes have a planar structure.

2. Transition State. The transition state (AT) is characterized by an irregular pentagonal cyclic structure and by a long-range interaction between the fragments OH and HCNH (Figure 2). The imaginary frequency is 264.5i cm^{-1}, and the associated reaction vector corresponds to a rocking motion of the O4−H6 moiety between H3 and H5. The C, N, H3, H5, and O4 atoms are almost coplanar, H6 lying out of the plane ($\angle$H6O4H3C = −143.8°). The negative charge is localized on the OH fragment (92%). For the forward reaction, the transition state consists of a proton transfer from H_2O to HCN^- to form $[HCNH\cdots OH^-]^\ddagger$ with an already formed NH bond (r(NH5) = 1.043 Å, r(O4H5) = 2.156 Å). The spin density is mostly distributed on N (60%) with contributions of C and H3 atoms (17% and 13%, respectively). From the transition state, the product is obtained by H3 proton transfer from HCNH to OH^-. The overall process looks like a proton exchange between HCN and H_2O. Because the proton transferred on one side of the transition state is not the same as the one that is transferred on the other side, an isotope-exchange mechanism can be proposed from HDO.

The inequalities r(CH3) > r(NH5) and r(O4H3) < r(O4H5) for the formed and broken bonds on both sides of the transition state indicate a structure closer both in geometry and energy to the product than the reactant. All of the stationary points on the PES are characterized by interactions between an open-shell structure and a closed-shell one (anion−molecule interaction for the minima and radical−anion interaction in the transition structure).

B. Discussion of the Mechanism. The reaction profile is presented in Figure 3. Among the mechanisms proposed in section II, the capture from vibrationally excited species is not likely to occur because internally excited complex (S) would dissociate into fragments. The capture of an electron must then occur directly from complex (S) in its fundamental vibrational levels; the first resonant species $(S)^-$ that results in an electron attachment into a π^*_{CN} orbital has a calculated attachment energy of 2.40 eV at our MRCI level. (For comparison, our calculated electron attachment energy for the first resonant state of a bare HCN resulting in an attachment into a π^*_{CN}-type orbital is 2.36 eV versus an experimental value of 2.30 eV.[60]) If the anion $(S)^-$ is long-lived enough, then the excess energy gained upon initial attachment would be redistributed into internal modes. One might wonder which modes can be activated by this capture. We know from previous studies that the first resonant state of HCN that corresponds to capture into a π^*_{CN}-type orbital can lead to a metastable bent molecule HCN^-.[60−62] Because the electronic capture for the formation of the first resonant state of (S) is in the same type of orbital as for the isolated monomer HCN, one can assume that the energy that is gained would be partially distributed in the $\angle$HCN bending mode. The other activated mode is the intermolecular stretching mode N···H5 as a result of the strong anion−molecule interaction that develops in the anionic complex and illustrated by the large anionic complexation energy for (AR), 0.63 eV. The redistribution of the excess energy in the initial structure

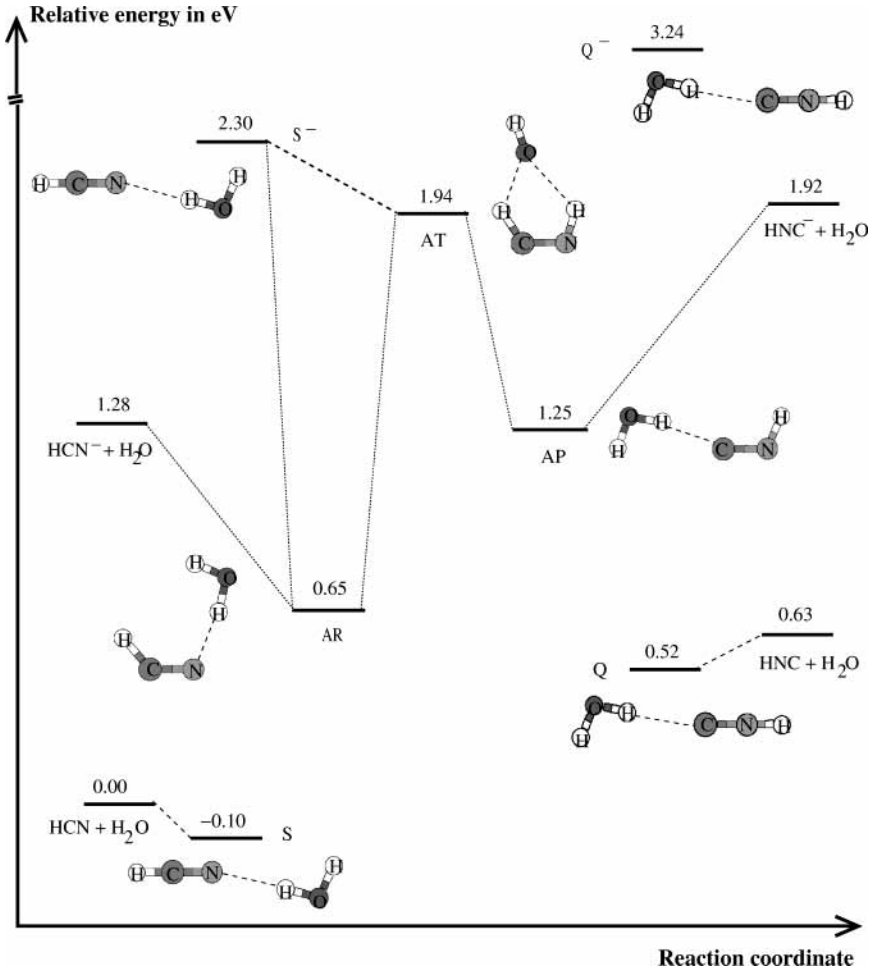

Figure 3. Reaction profile for the hydrated anionic isomerization calculated at the CCSD(T)/6-311+G(3df,2p)//MP2/6-311+G** + ZPE[MP2/6-311+G**] level and including BSSE corrections. The electron attachment energies for complexes (S) and (Q) are calculated at the MRCI/6-31+G** level. The relative energies are defined with respect to HCN + H_2O in electronvolts.

TABLE 1: Selected Scaled Frequencies Calculated at the MP2/6-311+G Level and Stabilization Energies (Complexation Energy or Vertical Detachment Energy VDE) Calculated at the CCSD(T)/6-311+G(3df,2p)//MP2/6-311+G** + ZPE[MP2/6-311+G**] Level (Including BSSE Corrections) for All Considered Species**

species	frequencies[a] (cm^{-1}) ν(CN)[b]	ν(XH)[c]	ν_s(OH)	stabilization energy (eV)
HCN	2015.8	3307.8		
HNC	2014.9	3642.3		
HCN^-	2220.6	1770.5		
HNC^-	1625.6	2684.9		
H_2O			3687.9	
HCN···HOH (S)	2031.5 (16)	3305.8 (−2)	3655.2 (−33)	0.10
HNC···HOH (Q)	2037.7 (23)	3640.4 (−2)	3631.0 (−57)	0.11
H_2O···HCN (R)	2013.0 (−3)	3203.5 (−104)	3679.3 (−9)	0.12
H_2O···HNC (P)	2014.1 (−1)	3352.7 (−290)	3677.4 (−10)	0.20
HCN^-···HOH (AR)	2194.6 (179)	2009.7 (−1298)	2979.9 (−708)	0.63
HNC^-···HOH (AP)	1715.1 (−300)	2779.7 (−863)	3072.5 (−615)	0.67
HCN + e^-				−0.68
HNC + e^-				−0.75
HCN···HOH + e^-				0.28
HNC···HOH + e^-				0.06
[HNCH···OH] + e^-				1.85[d]

[a] Frequency shift with respect to those of free fragments are given in parentheses. [b] Unscaled frequencies; see ref 11. [c] X = C for structures with a HCN moiety; X = N for structures with HNC. [d] VDE for the anionic transition state.

$(S)^-$ is thus mostly in the ∠HCN bending mode and the N···H5−O asymmetric stretching mode and can lead to the geometry of the barrier (AT) after the total transfer of the proton between the negatively charged nitrogen-atom end and the oxygen, thus looking like a dissociative attachment mechanism. As the energy redistribution occurs, the electron becomes thermodynamically bound since both the complex (AR) and the transition state structures have a positive vertical detachment energy. (See VDEs in Table 1.) The transfer of the excess energy into these modes therefore stabilizes the anionic structure by preventing electron detachment. On the product side of the barrier, the hydrated anionic hydrogen isocyanide structure is

TABLE 2: Scaled Frequencies (cm^{-1}) Calculated at the MP2/6-311+G Level for Complexes $HCN^-\cdot H_2O$ and $HNC^-\cdot H_2O$**

	$HCN^-\cdot H_2O$ (AR)		$HNC^-\cdot H_2O$ (AP)	
ν(OH)	3737.9	2979.9	3745.2	3072.5
ν(CN)	2194.6[a]		1715.1[a]	
ν(CH/NH)	2009.7		2779.7	
δ(HOH)	1631.6		1623.8	
δ(HCN/HNC) in plane	1033.5		938.4	
δ(HCN/HNC) out of plane	347.4		241.4	
ν	897.3	470.6	853.7	380.4
	240.1	144.1	200.7	92.8
	85.8		61.2	

[a] Unscaled frequencies; see ref 11.

formed after the transfer of the H3 hydrogen between C and O. The excess internal energy can be dissipated by the formation of the separated $HNC^- + H_2O$ with negligible internal and kinetic energy; rapid detachment of the electron will form neutral HNC. We can notice from Table 1 that complex (AR) has a positive VDE of 0.28 eV whereas a negative VDE of −0.68 eV is obtained for the HCN optimized anionic geometry, indicating the transient nature of the monomolecular bent HCN^-, at least for its ground vibrational state. This calculated increase in VDE due to the effect of a solvent molecule is consistent with the observation of Han et al.[63] in the series $[CO_2\cdot(\text{pyridine})_{n=1-6}]^-$.

Thus, under the assumption that the resonant $(S)^-$ complex has a sufficient lifetime, there exists a proton-exchange mechanism between the two moieties of the anionic structure that can finally lead to the HNC isomer.

V. Concluding Remarks

We have proposed a mechanism for the isomerization of HCN that takes into account the hydrated nature of the cometary environment and supposes an interaction with a cold electron in the inner cometary plasma region.[5−7] The transfer of the excess energy gained upon the capture of an electron into internal modes (as observed for HCN monomer) can lead to the formation of intermediate or transitory species with positive VDEs (structures (AR) or (AT), respectively), which can yield the separated HNC^- (subsequently decaying into HNC) and H_2O with very little excess energy for these products. This mechanism is relevant to a low-density medium where HCN is likely to exist in a hydrated form, thus in cometary atmospheres but also in interstellar clouds. Indeed, nitriles and isonitriles have been detected on the icy mantles of grains in interstellar clouds.[64−66] Since water ice is the main volatile of these grain mantles, UV processing can sublime the mantle material and form hydrated HCN complexes. Complex (S) can be formed and can subsequently interact with ambient electrons according to such a mechanism. Another final important aspect of this mechanism is a possible hydrogen/deuterium isotopic exchange between HCN and HDO to form DNC.

References and Notes

(1) Krishna, S. K. *Physics of Comets*; World Scientific Publishing Company: Singapore, 1986.

(2) Boice, D. C.; Huebner, W. F.; Keady, J. *J. Geophys. Res. Lett*. **1986**, *13*, 381.

(3) Irvine, W. M.; Morvan, D. B.; Lis, D. C.; Matthews, H. E.; Biver, N.; Crovisier, J.; Davies, J. K.; Dent, W. R. F.; Gautier, D.; Godfrey, P. D.; Keene, J.; Lovell, A. J.; Owen, T. C.; Phillips, T. G.; Rauer, H.; Schloerb, F. P.; Senay, M.; Young, K. *Nature* **1996**, *383*, 418.

(4) Irvine, W. M.; Bergin, E. A.; Dickens, J. E.; Jewitt, D.; Lovell, A. J.; Matthews, H. E.; Schloerb, F. P.; Senay, M. *Nature* **1998**, *393*, 547.

(5) Gringauz, K. I.; Gombosi, T. I.; Remizov, A. P.; Apathy, I.; Szemerey, I.; Verigin, M. I.; Denchikova, L. I.; Dyachkov, A. V.; Keppler, E.; Klimenko, I. N.; Richter, A. K.; Somogyi, A. J.; Szego, K.; Szendro, S.; Tatrallyay, M.; Varga, A.; Vladimirova, G. A. *Nature* **1986**, *321*, 282.

(6) Kozyra, T. E. C. J. U.; Nagy, A. F.; Gombosi, T. I.; Kurtz, M. *J. Geophys. Res*. **1987**, *92*, 7341.

(7) Korosmezey, A.; Cravens, T. E.; Gombosi, T. I.; Nagy, A. F.; Mendis, D. A.; Szego, K.; Gribov, B. E.; Sagdeev, R. Z.; Shapiro, V. D.; Shevchenko, V. I. *J. Geophys. Res*. **1987**, *92*, 7331.

(8) Gutowsky, H. S.; Germann, T. C.; Augspurger, J. D.; Dykstra, C. E. *J. Chem. Phys*. **1992**, *96*, 5808.

(9) Heikkilä, A.; Pettersson, M.; Lundell, J.; Khriachtchev, L.; Räsänen, M. *J. Phys. Chem. A* **1999**, *103*, 2945.

(10) Rivelino, R.; Canuto, S. *Chem. Phys. Lett*. **2000**, *322*, 207.

(11) Gardebien, F.; Sevin, A. *J. Phys. Chem. A* **2003**, *107*, 3925.

(12) Schulz, G. J. *Rev. Mod. Phys*. **1973**, *45*, 423.

(13) Chen, J. C. Y. *Phys. Rev*. **1966**, *148*, 66.

(14) Christophorou, L. G.; Stockdale, J. A. D. *J. Chem. Phys*. **1968**, *48*, 1956.

(15) McCurdy, C. W.; Mowrey, R. C. *Phys. Rev. A* **1982**, *25*, 2529.

(16) Walsh, A. D. *J. Chem. Soc*. **1953**, 2260.

(17) Goldstein, E.; Segal, G. A.; Wetmore, R. W. *J. Chem. Phys*. **1978**, *68*, 271.

(18) Rajzmann, M.; Spiegelmann, F.; Malrieu, J. P. *J. Chem. Phys*. **1988**, *89*, 433.

(19) Benassi, R.; Bernardi, F.; Bottoni, A.; Robb, M. A.; Taddei, F. *Chem. Phys. Lett*. **1989**, *161*, 79.

(20) Nestmann, B. M.; Peyerimhoff, S. D. *J. Phys. B* **1985**, *18*, 4309.

(21) Walsh, M. B.; King, R. A.; Schaefer, H. F., III. *J. Chem. Phys*. **1999**, *110*, 5224.

(22) Saeki, M.; Tsukuda, T.; Iwata, S.; Nagata, T. *J. Chem. Phys*. **1999**, *111*, 6333.

(23) Surber, E.; Ananthavel, S. P.; Sanov, A. *J. Chem. Phys*. **2002**, *116*, 1920.

(24) Surber, E.; Sanov, A. *J. Chem. Phys*. **2002**, *116*, 5921.

(25) Moller, C.; Plesset, M. S. *Phys. Rev*. **1934**, *46*, 618.

(26) Urban, M.; Noga, J.; Cole, S. J.; Bartlett, R. J. *J. Chem. Phys*. **1985**, *83*, 4041.

(27) Bartlett, R. J.; Watts, J. D.; Kucharski, S. A.; Noga, J. *Chem. Phys. Lett*. **1990**, *165*, 513.

(28) Walter, C. W.; Smith, K. A.; Dunning, F. B. *J. Chem. Phys*. **1989**, *90*, 1652.

(29) Kalamarides, A.; Marawar, R. W.; Ling, X.; Walter, C. W.; Lindsay, B. G.; Smith, K. A.; Dunning, F. B. *J. Chem. Phys*. **1990**, *92*, 1672.

(30) Kalamarides, A.; Marawar, R. W.; Durham, M. A.; Lindsay, B. G.; Smith, K. A.; Dunning, F. B. *J. Chem. Phys*. **1990**, *93*, 4043.

(31) Thoss, M.; Domcke, W. *J. Chem. Phys*. **1998**, *109*, 6577.

(32) Knapp, M.; Echt, O.; Kreisle, D.; Mark, T. D.; Recknagel, E. *Chem. Phys. Lett*. **1986**, *126*, 225.

(33) Frisch, M. J.; Trucks, G. W.; Schlegel, H. B.; Scuseria, G. E.; Robb, M. A.; Cheeseman, J. R.; Zakrzewski, V. G.; Montgomery, J. A., Jr.; Stratmann, R. E.; Burant, J. C.; Dapprich, S.; Millam, J. M.; Daniels, A. D.; Kudin, K. N.; Strain, M. C.; Farkas, O.; Tomasi, J.; Barone, V.; Cossi, M.; Cammi, R.; Mennucci, B.; Pomelli, C.; Adamo, C.; Clifford, S.; Ochterski, J.; Petersson, G. A.; Ayala, P. Y.; Cui, Q.; Morokuma, K.; Malick, D. K.; Rabuck, A. D.; Raghavachari, K.; Foresman, J. B.; Cioslowski, J.; Ortiz, J. V.; Stefanov, B. B.; Liu, G.; Liashenko, A.; Piskorz, P.; Komaromi, I.; Gomperts, R.; Martin, R. L.; Fox, D. J.; Keith, T.; Al-Laham, M. A.; Peng, C. Y.; Nanayakkara, A.; Gonzalez, C.; Challacombe, M.; Gill, P. M. W.; Johnson, B. G.; Chen, W.; Wong, M. W.; Andres, J. L.; Head-Gordon, M.; Replogle, E. S.; Pople, J. A. *Gaussian 98*, revision A.7; Gaussian, Inc.: Pittsburgh, PA, 1998.

(34) Frisch, M. J.; Pople, J. A.; Binkley, J. S. *J. Chem. Phys*. **1984**, *80*, 3265.

(35) Krishnan, R.; Binkley, J. S.; Seeger, R.; Pople, J. A. *J. Chem. Phys*. **1980**, *72*, 650.

(36) Clark, T.; Chandrasekhar, J.; Spitznagel, G. W.; Schleyer, P. v. R. *J. Comput. Chem*. **1993**, *4*, 294.

(37) Redmon, L. T.; Purvis, G. D., III; Bartlett, R. J. *J. Chem. Phys*. **1980**, *72*, 986.

(38) Buijse, M. A.; Baerends, E. J. *Density Functional Theory of Molecules, Clusters, and Solids*; Kluwer Academic Publishers: Dordrecht, The Netherlands, 1995.

(39) Boys, S. F.; Bernardi, F. *Mol. Phys*. **1970**, *19*, 553.

(40) Mayer, P. M.; Parkinson, C. J.; Smith, D. M.; Radom, L. *J. Chem. Phys*. **1998**, *108*, 604.

(41) Scott, A. P.; Radom, L. *J. Phys. Chem*. **1996**, *100*, 16502.

(42) Lee, T. J. *J. Am. Chem. Soc*. **1989**, *111*, 7362.

(43) Novakovskaya, Y. V.; Stepanov, N. F. *Int. J. Quantum Chem*. **1997**, *63*, 737.

(44) Chen, H. Y.; Sheu, W. S. *J. Chem. Phys*. **1999**, *110*, 9032.

(45) Clark, T.; Chandrasekhar, J.; Spitznagel, G. W.; v. R. Schleyer, P. *J. Comput. Chem*. **1983**, *4*, 294.
(46) Jursic, B. S. *Int. J. Quantum Chem.* **1999**, *72*, 571.
(47) Chandrasekhar, J.; Andrade, J. G.; v. R. Schleyer, P. *J. Am. Chem. Soc.* **1981**, *103*, 5609.
(48) Cremaschi, P.; Morosi, G.; Simonetta, M. *J. Mol. Struct*. **1981**, *85*, 397.
(49) Kollmar, H. *J. Am. Chem. Soc*. **1978**, *100*, 2665.
(50) Fukui, K. *J. Phys. Chem.* **1970**, *74*, 4161.
(51) Fukui, K. *Acc. Chem. Res.* **1981**, *14*, 363.
(52) Gutsev, G. L.; Bartlett, R. J.; Compton, R. N. *J. Chem. Phys.* **1998**, *108*, 6756.
(53) Pacansky, J.; Wahlgren, U.; Bagus, P. S. *J. Chem. Phys*. **1975**, *62*, 2740.
(54) Compton, R. N.; Reinhardt, P. W.; Cooper, C. D. *J. Chem. Phys*. **1975**, *63*, 3821.
(55) MOLPRO is a package of ab initio programs written by Werner, H. J. and Knowles, P. J. with contributions from Almlof, J.; Amos, R.; Deegans, M. J. O.; Elbert, S. T.; Hampel, C.; Meyer, W.; Peterson, K.; Pitzer, R.; Stone, A. J.; Taylor, P. R.
(56) Werner, H. J.; Knowles, P. J. *J. Chem. Phys*. **1988**, *89*, 5803.
(57) Knowles, P. J.; Werner, H. J. *Chem. Phys. Lett*. **1988**, *145*, 514.
(58) Werner, H. J.; Reinsch, E. A. *J. Chem. Phys*. **1982**, *76*, 3144.
(59) Werner, H. J. *Adv. Chem. Phys*. **1987**, *59*, 1.
(60) Jain, A.; Norcross, D. W. *Phys. Rev. A* **1985**, *32*, 134.
(61) Jain, A.; Norcross, D. W. *J. Chem. Phys*. **1986**, *84*, 739.
(62) Ng, L.; Balaji, U.; Jordan, K. D. *Chem. Phys. Lett*. **1983**, *101*, 171.
(63) Han, S. Y.; Chu, I.; Kim, J. H.; Song, J. K.; Kim, S. K. *J. Chem. Phys*. **2000**, *113*, 596.
(64) Sandford, S. A. *Astron. Inf. Spectrosc*. **1993**, *41*, 181.
(65) Bernstein, M. P.; Sandford, S. A.; Allamandola, L. J.; Chang, S. *Astrophys. J*. **1995**, *454*, 327.
(66) Whittet, D. C. B.; Schutte, W. A.; Tielens, A. G. G. M.; Boogert, A. C. A.; de Graauw, T.; Ehrenfreund, P.; Gerakines, P. A.; Helmich, F. P.; Prusti, T.; van Dishoeck, E. F. *Astron. Astrophys*. **1996**, *315*, L357.